

LOEW: ELECTRON LINAC INSTABILITIES

ELECTRON LINAC INSTABILITIES*

G. A. Loew

Stanford Linear Accelerator Center
Stanford, CaliforniaSummary

This paper attempts to summarize the present state of understanding of electron linac instabilities which result in beam loss along the accelerator. The major emphasis is placed on the type of instability which is caused by cumulative interaction of the beam with a multisection accelerator, as distinguished from the effect observed in short high-current accelerators where the instability is due to local regenerative interaction. The manifestations of the effect are first described and physical models are proposed. The properties of the HEM₁₁ mode which is responsible for the instability are discussed in detail. Following, a short summary of the Panofsky theory is presented to illustrate various scaling laws which have been verified experimentally on the SLAC accelerator. Measured results are also compared with a detailed computer study made by R. Helm and agreement is generally found to be very good. After the discussion of beam break-up gain, a few conjectures are presented on the possible starting mechanisms of the effect. In conclusion, the program presently underway at SLAC to increase the current

threshold of the instability is outlined and early results of this program are presented.

Introduction

During the past year, there has been a considerable upsurge of interest in the problem of electron linac instabilities. While manifestations of the phenomenon known alternatively as beam break-up, beam blow-up or pulse shortening, had been observed¹ as early as 1957 in various short commercially built linacs, the problem has now generated concern throughout the field because it appears that the entire new generation of long and high duty cycle linear accelerators is affected by some form of instability. This fact, which became particularly evident at the 1966 Linear Accelerator Conference held at Los Alamos last October, is illustrated in Table I. This table, while perhaps incomplete, attempts to summarize the various types of instabilities, their thresholds, the categories of machines which are affected and the respective theories and remedies which have been proposed. Prior to 1966, with the exception of the Kharkov and Desy linacs, only the

Table I
Known Types of Linac Instabilities

Mode	Mechanism	Pulse Length	Current Threshold	Examples of Accelerators	Theory	Remedies
Transverse deflecting H _{EM} ₁₁	Regenerative Backward-Wave Oscillator	~1 to ~10 μ sec	≥ 500 mA	Commercial Accelerators (Hughes, Arco, Varian, Metropolitan Vickers, Vickers Armstrong)	P. B. Wilson G. H. H. Cheng R. Gluckstern R. Helm	Solenoidal focusing Modify structure
				Kharkov	W. Panofsky R. Helm	Modify structure
	Multisection Amplifier	< 2 μ sec (Transient)	5mA < i < 100mA	SLAC	A. Sessler R. Gluckstern	Quadrupole focusing
				MIT	R. Helm	Stagger and modify sections
		~10 μ sec (Transient to Steady-State)	Unknown	ALS (Saclay)	H. Lebouet R. Gluckstern	Solenoidal and quadrupole focusing
				LASL (Proton Acc.)	W. Visscher R. Gluckstern	Focusing
Coupling with resistive wall		c - w	Unknown	Stanford Superconducting Accelerator	W. Panofsky R. Helm	Feedback Focusing
		-	Several Amperes	Not yet built	A. Sessler P. Morton	Unknown

*Work supported by the U.S. Atomic Energy Commission

regenerative type of beam break-up had been clearly recognized. In this respect, it can be stated that the SLAC accelerator where the multisection type of break-up was identified shortly after turn-on (April 1966), has served as the longest guinea-pig in the world. Accelerators such as the MIT, ALS (Saclay), LASL and superconducting machines will no doubt profit from this experience even though the applicable theories and remedies may not be entirely the same. The resistive wall instability which should not plague any of the existing or planned linacs, is mentioned here for completeness because it will probably constitute the next stumbling block if the present HEM_{11} transverse mode thresholds can be superseded.

While the title of this paper would clearly require that all the above instabilities be discussed here, both the lack of space and the present incompleteness of knowledge make such a task impossible. For this reason, after a brief comparison of the regenerative and the cumulative instabilities, this report will be devoted almost exclusively to the SLAC type of beam break-up. Furthermore, because of the difficulty in summarizing the existing analytic and computer theories^{1,2,3,4}, this paper will lean heavily on physical models and experimental evidence. Where necessary, use will be made of the Panofsky theory even though, admittedly, it does not take detailed account of all the physical facts such as the interaction mechanism and lumped quadrupole focusing. In turn, for a more exact comparison between theory and experiment, use will be made of the results of the Helm computer studies.

To guide the reader, the main paragraphs of this report are listed below:

- Physical manifestation of beam break-up
- Models for regenerative and cumulative break-up
- Characteristics of the HEM_{11} mode in the SLAC disk-loaded waveguide
- Theory vs experiments on multisection beam break-up gain
- Discussion of noise sources
- Remedies and expectations

Physical Manifestation of Beam Break-Up

While the mechanism of beam break-up may vary from one accelerator to another, the basic physical manifestation of the phenomenon as shown in Fig. 1a is the same for all. As seen from the three video pulses, the injected beam pulse length, shown here to be 1.5 μsec for the top pulse, is shortened erratically when the beam current is increased above a certain value. The shortening becomes more pronounced as the current from the injector is increased. In the case of a multi-section accelerator, this pattern of pulses can be observed at any location along the accelerator and the onset

of beam break-up is determined by the beam current transmitted through that point. Under such conditions, the beam profiles along the SLAC accelerator appear as shown in Fig. 1b. The ordinates of the dots represent the amount of charge transmitted past the end of each of the thirty accelerator sectors. In the lower trace (17 mA), the beam current from the injector is at a level below the break-up threshold for this particular set of energy, pulse length and focusing conditions and no current is lost along the accelerator. In the upper trace (52 mA), the injected current has been increased to a level far above the break-up threshold. As can be seen, the current transmitted past Sector 8 becomes erratic and an increasingly large fraction of the electron bunches is lost to the accelerator and collimator walls. Those bunches which get beyond Sector 8 correspond to increasingly earlier parts of the injected pulse.

Models for Regenerative and Cumulative Break-Up

As stated above, beam break-up was first discovered in short high current accelerators. After a period of bewilderment, workers in the field⁵⁻⁹, both in England and in the U.S.A., began to recognize the similarity of the phenomenon with backward-wave oscillations observed and generated in microwave tubes. Careful investigations¹⁰ of the disk-loaded accelerator structure showed that, above the TM_{01} accelerating mode, there are indeed many other propagating modes, some of which exhibit transverse deflecting properties. The first one is "TM₁₁-like" and will hereafter be called HEM_{11} because of its mixed "E" and "H" nature. Its frequency, $\omega-\beta$ diagram, Q and interaction impedance differ from one accelerator structure to another but its frequency ratio to the fundamental accelerator frequency is roughly constant and in the neighborhood of 3/2. The longitudinal electric field is zero and changes sign on the axis. Now that many microwave experiments have been carried out¹¹, it appears that a judicious design of the structure can minimize its interaction properties with the beam. Further discussion of these properties will appear in the next paragraph.

Both the regenerative and cumulative types of beam break-up are caused by interaction with the HEM_{11} -mode. Both instabilities start from noise which consists of or results in a small transverse modulation of the electron bunches at the break-up frequency. However, the growth mechanisms are different. Regenerative break-up occurs in one section. Its mechanism is illustrated in Fig. 2a. It requires a negative group velocity structure for oscillation build-up. Consider a noise-generated HEM_{11} wave traveling with a phase velocity in the same direction as the electrons but slightly slower than them so that they slip ahead by 180° in their travel along the accelerator section. In the first half, the phase of the wave is such that the force on the electron bunches is strongly deflecting. Depending on their phase and the plane of polarization of the wave, they are deflected to either one side or the

LOEW: ELECTRON LINAC INSTABILITIES

other in that plane. As they get deflected, they also slip ahead in phase and in the second half of the section, they find themselves in a longitudinally decelerating field to which they give up energy. Because of the backward-wave characteristic of the mode, this energy travels back upstream where it reinforces the original deflecting field. Above a certain starting current and pulse length, the process becomes regenerative¹² and both the field and the deflection grow exponentially. As a result, the beam is lost.

In contrast, the cumulative, multisection type of break-up is illustrated in Fig. 2b. Here, because of the same small initial transverse modulation of the electron bunches or initial cavity excitation, the early accelerator sections undergo individual oscillations at some HEM_{11} resonant frequency. As a result, the next electron bunches which see this field receive an additional amount of transverse momentum which over a given distance translates itself into displacement modulation. This modulation further excites the resonant fields in the downstream cavities and these, in turn, deflect the bunches even more until finally they scrape the accelerator walls. Since the isolated resonances within individual sections are due to multiple reflections, the waves need not be of the backward type. The mechanism is illustrated in greater detail in Fig. 3 where, for simplicity, each accelerator section is lumped into a single cavity and snapshots of the electric field are taken at the time of passage of the bunches. The transverse arrows indicate the magnitude of the corresponding transverse momentum impulse. The history of a finite number of bunches is followed during their passage through 3 cavities with the ensuing resonant field build-up. It should be noticed that individual bunches can be at any phase with respect to the field. Independently of the initial phase, the asymptotic phase for maximum build-up is 45° , such that the bunches are half-way between the phase of maximum momentum transfer and maximum field excitation. Within each beam pulse, the effect is coherent and cumulative as a function of length and time. As the accelerator current is increased, break-up at SLAC appears first in the vertical direction because the Q of the mode is slightly higher in the plane perpendicular to the couplers. At higher current, however, the orientation of the break-up plane becomes isotropic and random from pulse to pulse.

Characteristics of the HEM_{11} Mode in the SLAC Disk-Loaded Waveguide

As discussed above, the frequency at which the HEM_{11} mode gets excited in the regenerative case, is approximately such that a " π " phase slippage takes place between the wave and the electron bunches over the section length^{1,12}. In the multi-section cumulative case, the frequency depends on whatever resonances the beam can set up in the structure. The characteristics of the SLAC constant-gradient structure have been extensively discussed elsewhere^{13,11} and only the essential properties relevant to these resonances will be

reviewed here. The accelerator mode is of the TM_{01} type with $2\pi/3$ phase shift per cavity at 2856 MHz. The constant-gradient design is such that, over each ten-foot section consisting of 86 cavities of decreasing cross-section from input to output, the group velocity decreases linearly in the range $0.0204 > v_g/c > 0.0061$. Because of these tapered dimensions, for any frequency other than 2856 MHz, the phase shift per section changes from cavity to cavity. Brillouin diagrams for specific cavities can be obtained with equivalent cavity stacks. Experimental data for the HEM_{11} mode in cavities at three different locations are shown in Fig. 4.

The first resonant frequency at which beam break-up has been observed at the present operating currents (< 100 mA) is 4139.6 MHz, roughly 4140 MHz. Since the electrons are bunched at 2856 MHz, the growing sine-wave representing the envelope of their displacement appears not only at 4140 MHz but also at the difference frequency, $4140 - 2856 = 1284$ MHz. It also appears at the difference between the third harmonic of 2856 minus 4140, namely 4428 MHz and at $4428 - 2856 = 1572$ MHz (etc.). Hence, while the basic microwave interaction takes place only at 4140 MHz, the other frequencies are always present on the beam. They can be detected by means of microwave probes and can also be used to precipitate or sharpen the break-up by artificially stimulating the beam at the beginning of the machine with an external source. The mechanism by which the first and higher resonances can be excited is understood by further examining Fig. 4. At 4139.6 MHz, the phase shift of the first cavity beyond the coupler is 0.765π . As the wave at this frequency progresses along the guide, the phase shift per cavity reaches π and then becomes cut-off. It has been found, both theoretically and experimentally, that the lowest resonance occurs when the phase shift through the first 8 to 10 cavities adds up to a multiple of π . Fig. 5 shows that there is excellent agreement for the first three resonances between the computer calculations carried out by Helm¹ (Fig. 5b) and the VSWR measured at the input of the structure (Fig. 5a). The amplitude for the first mode has also been measured by means of a bead perturbation test and again, good agreement has been found. The phase angle is plotted for the wave with respect to a relativistic beam. The fact that it is not zero can be understood since in Fig. 4, the crossover of the $v_p = c$ line allows only quasi-synchronism.

Another characteristic of the structure is that break-up for low currents (~25 ma) and long pulses (1.6 μsec) occurs only in the vertical plane, perpendicular to the plane of the couplers. It is only after increasing the beam current above the vertical threshold in a ratio of approximately 3 to 2 that the break-up plane for a 1.6 μsec pulse becomes random. This fact can be understood because the Q is higher in the vertical direction where no coupler leakage occurs. It appears that the value of Q_0 is of the order of 8000 and that Q_L , the loaded Q in the horizontal plane, is roughly two-thirds of this value. The one-way

travel time of the resonant wave is of the order of 50 nanosec. Hence, for very short high current injector pulses, the beam still breaks up in one plane but since there is no time for resonant build-up, the orientation of the plane becomes random from pulse to pulse. It is also probable that there is a slight difference between the horizontal and vertical resonant frequencies. For this reason, the VSWR minima in Fig. 5a exhibit double kinks. As to the shunt impedance which will be discussed in the next paragraph, it appears to be close to $12.5 \text{ M}\Omega/\text{meter}$.

Theory vs Experiments on
Multisection Beam Break-Up Gain

There are presently two theoretical approaches to the multisection beam break-up problem. One is analytic^{2,3} and can yield closed asymptotic solutions for certain cases. However, it assumes only one resonant mode, it is based on

a simplified model where each accelerator section is lumped in a single cavity and it can only take into account focusing if the focusing force is spread out along z (rather than being lumped as is the case with real quadrupole lenses). The other uses a computer calculation^{1,14}. Here, the representation of the accelerator is much more exact since a coupled cavity model can be used and lumped focusing can be handled by means of the usual beam transport program. In addition, these calculations have the virtue that the initial conditions can be easily modified and their effect tested. The purpose of this section is to show the general dependence of the rate of growth on such variables as time (t), distance (z), current (i), energy gradient (γ') and betatron wavelength (λ_B) and to compare some of the theoretical results and computer calculations with experimental results.

The Panofsky theory² is outlined in Table II. A solution of equation (4) in terms of specific

Table II

Summary of Panofsky Theory

Transverse impulse received
by electron passing through
interaction region

$$\Delta p_x = \frac{ie}{\omega} \int \frac{\partial E_z}{\partial x} dz \quad (1)$$

Equation of motion

$$\underbrace{\frac{\partial}{\partial z} (\gamma \frac{\partial x}{\partial z})}_{\text{Momentum Change}} = -\gamma k_B^2 x + \underbrace{\frac{ie}{\omega m_0 c L} \int \frac{\partial E_z}{\partial x} dz}_{\text{Transverse Impulse}} \quad (2)$$

Cavity field equation

$$\underbrace{\frac{\partial}{\partial t} \int \frac{\partial E_z}{\partial x} dz}_{\text{Loss}} = -\underbrace{\frac{\omega}{2Q} \int \frac{\partial E_z}{\partial x} dz}_{\text{Beam Coupling}} - I_o x \frac{CL \omega m_0 c}{e} \quad (3)$$

Coupled equation

$$\left(\frac{\partial}{\partial t} + \frac{\omega}{2Q} \right) \left[\frac{\partial}{\partial z} (\gamma \frac{\partial x}{\partial z}) + \gamma k_B^2 x \right] = -ic I_o x \quad (4)$$

Asymptotic solution without
focusing ($k = 0$) and phase
variation

$$x = x_0 \exp \left\{ 1.64 (C I_o t)^{1/3} \left(\int_{z_0}^z \frac{dz}{[\gamma(z)]^{1/2}} \right)^{2/3} - \frac{\omega}{2Q} t - \frac{1}{4} \log \frac{\gamma}{\gamma_0} \right\} \quad (5)$$

Definitions:

$\gamma m_0 c^2$ = electron energy

I_o = beam current

ω = frequency

$k_B = \frac{2\pi}{\lambda_B}$ = betatron propagation constant

x = transverse electron coordinate

L = distance between interaction regions

Q = cavity loss factor

$C = \frac{e}{m_0 c^2} \frac{cr_t l_1}{LQ} \frac{\omega^2}{2c^2}$ where r_t = transverse shunt impedance

c = velocity of light

l_1 = effective interaction length

LOEW: ELECTRON LINAC INSTABILITIES

starting conditions cannot be obtained in closed analytic form. Nor has it been obtained so far for the case of medium or strong focusing which applies under most operating conditions. On the other hand, it is possible to evaluate the function $x(z, t)$, first by assuming an adiabatic variation of γ with z (WKB approximation) to get a general solution of (4) and then by generating an asymptotic solution by the method of steepest descent. This asymptotic solution is given in (5). The term x_0 which represents the initial conditions will be discussed in the next section. The first term in the exponent is dominant and for most practical cases is of the order of 20. The second is the decay term and its magnitude for a typical SLAC pulse length (1.5 μ sec) is of the order of 2. The $\log [\gamma/\gamma_0]^{-1/4}$ term and a fourth term of the form

$$\log \left[\left(\frac{I_0}{e} \right)^{-1/6} t^{5/6} \left(\frac{1}{L} \int_{z_0}^z \frac{dz}{[\gamma(z)]^{1/2}} \right)^{-1/3} \right] \quad (6)$$

which has been left out for simplicity, vary slowly with the parameters of interest. This can be seen since they appear in the form $e \log []$ and the parts in brackets simply act as multipliers of x_0 . Scaling laws on beam break-up gain can now be deduced for various cases:

a) For constant acceleration ($\gamma = \gamma' z$, $z \gg z_0$), the integral in the first term in the exponential can be evaluated. The beam will start to scrape the walls (I.D. = 1.7 cm) when

$$\frac{3\sqrt{3}}{2} \left(\frac{C I_0 t z}{\gamma'} \right)^{1/3} \sim 20. \quad (7)$$

This implies that to the extent that the other terms and focusing can be neglected, the transmitted charge I_{tot} is roughly conserved, and the plots of I_0 vs $1/z$ and γ' are straight lines. These results have been verified¹¹ and two examples are shown in Figs. 6a and 6b.

b) For acceleration up to $\gamma_1 = \gamma' z_1$ ($z_1 \gg z_0$) and coasting from there to z_2 , the exponent becomes

$$1.64 \left(\frac{C I_0 t}{\gamma_1} (z_1 + z_2)^2 \right)^{1/3} \sim 20. \quad (8)$$

A number of experiments for this case have also been carried out with only fair agreement.

In the presence of medium or strong focusing, the above scaling laws break down and one must resort to the computer programs. Experimental data can be taken and presented in a variety of ways. For example, it is possible to measure the beam break-up current at a given z and t while varying the energy gradient and the quadrupole current. The data can then be plotted as a function of betatron phase shift $k_B S$ per sector of length S . The betatron wavelength can be

computed or measured experimentally from figures such as Fig. 7. A reasonable approximation can also be obtained from the expression

$$\cos k_B S = 1 - \frac{1}{2} \frac{S}{f} \quad (9)$$

where f is the focal length of the quadrupole doublets. Empirically, it has been found that this relation can be written approximately as

$$\cos k_B S = 1 - 0.72 \left(\frac{\Delta i}{E_S} \right)^2 \frac{s}{640} \quad (10)$$

where Δi is the quadrupole current increment per sector in amperes and E_S is the energy increment per sector in MeV.

Fig. 8 is a plot of beam break-up currents as a function of $k_B S$ at Sector 19. It is seen that the agreement with the computer calculation is excellent. The fact that the graphs are very close to straight lines for $k_B S < 0.4\pi$ suggests that a reasonable fit for the Panofsky solution (Eq. 5) extended to the case of medium or strong focusing and constant γ' , could be of the form

$$\left(\frac{C I_0 t z}{\gamma'(k + \alpha)} \right)^{1/3} = \text{constant}. \quad (11)$$

In all these examples, it should be noticed that the term C contains r_t/Q which is simply a function of cavity geometry, independent of the losses.

Discussion of Noise Sources

The term x_0 in equation (5) has not been discussed so far. It represents the input to the multisection amplifier and depends on the starting conditions. As this paper is being written, there seem to be five competing contenders as noise sources at the beginning of the accelerator. They are illustrated in somewhat simplified form in Fig. 9. As will be seen below on the basis of theory, at least four of them appear to be of approximately the same order of magnitude. Experiments are being conducted to discover if one of them is dominant. Whether this is the case or not, it should be pointed out that it would take a significant reduction in noise power before the effect on the current threshold could become noticeable.

Hence, letting the dominant term in the exponential of equation (5) be called F , it can be shown that a reduction in noise power R in dB corresponds to a relative increase in beam break-up threshold

$$T = \left(1 + \frac{R_{dB}}{8.68F} \right)^3 \quad (12)$$

Thus, for example, letting $R \sim 20$ dB and $F \sim 20$, it is seen that $T = 1.39$, giving less than 40% improvement. We shall now discuss briefly the nature of each of the noise sources, by referring to Fig. 9.

Shock Excitation

While expression (5) is purely asymptotic, it has been possible to obtain a solution by iteration¹⁵, assuming an initial δ -function impulse at instant T , i.e. $x(z = z_0, t) = \delta(t-T)$. In their computer studies, Helm and Herrmannsfeldt¹⁴ have also studied the effect of various starting conditions. For example, they have found that once the cavity field configuration is assumed, it is enough to let the bunched beam be injected slightly off axis to get the build-up mechanism started. Specifically, they have found that if the beam is offset by 1 mm and has a rise time of several nanoseconds, the excitation is equivalent to an initial modulation in x of the order of 10^{-7} cm. With e-foldings corresponding to $\sim 10^7$ as have been assumed above and a limiting aperture radius of the order of 1 cm, this initial modulation would be sufficient. Experimentally, several conclusions would have to be drawn from this result. One is that the beam break-up threshold should be quite sensitive to misalignment or mis-steering in the beginning of the accelerator. While this fact has been observed, it has been difficult to measure it. In any case, the effect does not appear to be very strong. The second is that the threshold should be strongly dependent on gun pulse shape. Hence, intuitively, a slowly rising ramp pulse should yield a higher threshold than a square pulse containing the same total charge. Experiments of this type have been carried out but, again, perhaps because of the difficulties in obtaining clear-cut pulse shapes for comparison, the results have not been conclusive. A third consequence of this model is that if x_0 is linear with I_0 , the initial equivalent noise power must be quadratic with current. As will be shown in the next paragraph, it is not clear that this is the case.

Shot Noise

There are two ways in which shot noise from the gun can couple to the HEM_{11} mode. One is with the beam centered on axis but containing transverse modulation at the HEM_{11} frequency. The other, similar to shock excitation, is through longitudinal modulation at the HEM_{11} frequency with the beam line slightly off axis. The latter example had to be shown in Fig. 9 in an oversimplified way (one small bunch between two large ones) since it would have taken a larger number of bunches and many dots of different sizes to show modulation at 4140 MHz.

Using the usual formulas for temperature limited shot noise power in a bandwidth f/Q , these two effects can be lumped¹⁶ in the expression

$$\overline{x_0^2} = \frac{2e}{I_0} \frac{f}{Q} \left[\left(\frac{r}{2} \right)^2 + \delta^2 \right] \quad (13)$$

where f is the break-up frequency and r is the radius of the beam whose center of charge is offset by δ . Taking an equivalent lumped value for the bracket of $(1 \text{ mm})^2$, it is seen that x_0 is of the order of 10^{-6} cm, in strong competition with the shock excitation discussed above. Several con-

clusions can be drawn from this result. One is that the break-up threshold should change as the gun goes from temperature to space charge limited operation. Several experiments were carried out and indeed the break-up threshold was found to be increased by about 12% from the temperature to the space charge limited case. Unfortunately, under normal conditions, the gun is already operating under space charge limited conditions and no further improvement seems easily obtainable.

The other conclusion is that the noise power must be linear with injected current (as opposed to quadratic for shock noise). To test this idea, the following experiment was devised. At the 40 ft. point, downstream of the injector, power P_0 at 4140 MHz was injected into an in-line C-band cavity (for more details on this equipment, see Ref. 11). At the end of Sector 5, roughly 1600 ft. downstream, beam induced power P_5 was extracted from a similar cavity. In the absence of any external excitation, this induced power P_5 was measured for a given beam current. Then, the injected power P_0 was increased until P_5 was roughly doubled. This measurement was repeated over a range of beam currents. Although the experiment was difficult to perform and the data may be in error by as much as 50% because of the inherent instability of the induced pulse, that fraction of injected power P_0 which actually acts on the bunches must be of the same order of magnitude as the natural noise power carried by the beam. Hence, a relative, normalized measure of noise power can be inferred. The results are plotted in Fig. 10. Disregarding the uncertainties in the data, it appears that the noise power is linear with current rather than quadratic.

Finally, another observation should be mentioned. Referring back to Fig. 3, it can be seen that since the HEM_{11} frequency (4140 MHz) is close to the $3/2$ frequency (4284 MHz) of the accelerator bunch frequency (2856 MHz), every time a bunch goes through the middle of a cavity, the field has reversed itself by almost 180° (actually $\sim 162^\circ$). It takes roughly twenty bunches to return to the initial field condition. If now the beam is longitudinally modulated in such a way that it contains frequency harmonics which interact with the ringing frequency of the cavity, the threshold may be decreased. Such an experiment has been performed with the aid of an rf sweeper installed downstream of the gun for time-of-flight measurements. This rf sweeper lets only every 36th bunch into the accelerator. Under these conditions of sub-harmonic bunching, it has been found that the total transmitted current (or charge) below break-up threshold is only 40% of the current transmitted when the beam is modulated at 2856 MHz. It should be noted, however, that while this observation definitely shows that the starting noise is related to the current, it favors the hypothesis of shock rather than shot noise since the total current I_0 remains the same.

LOEW: ELECTRON LINAC INSTABILITIES

Thermal and Klystron Noise

While the above observations may all be correct, it is still possible that the dominant noise source stems from rf excitation. By calculation, the thermal excitation of the cavities is probably only one order of magnitude below the noise power corresponding to the above 10^{-7} cm modulation. On the other hand, it is very difficult to ascertain how much noise power is being generated by the klystrons and what fraction of it gets past the waveguide couplers and onto the beam. Numerous experiments have been performed. The insertion of low-pass filters at the input of the first klystrons has produced no effect. Nor has it been possible to detect beam break-up threshold changes as a function of klystron beam voltage in the first sections, although, admittedly, this experiment cannot be done over a wide range before the change in γ' , the energy gradient, begins to dominate. The output spectra of several types of SLAC klystrons have been investigated with some care. Unfortunately, it takes only fractions of milliwatts of injected power into the waveguide system (with all the unknown mismatches at 4140 MHz) to stimulate break-up. Hence, with 20 MW of klystron output power at 2856 MHz, measurements at 4140 MHz must be performed at least 100 dB below this level. These measurements are difficult because of the unknown frequency response of the high-power couplers for different waveguide modes and have so far been inconclusive. A program is presently underway at SLAC to build a few high power waveguide filters with an attenuation of at least 40 dB at 4140 MHz and 4428 MHz. If successful, these filters could be installed in the output waveguides of the first few klystrons with the hope that whatever power is being generated by these klystrons would be attenuated by another 40 dB. Only minor hope, however, is being held at the present time for this solution unless the filtering can be made effective over a very wide band to include the interaction with harmonics. In conclusion, it is clear that more work and ingenuity are still needed to obtain a definitive understanding of the beam break-up starting conditions and a possible reduction of their amplitude.

Remedies and Expectations

As discussed in the introduction, the problem of beam break-up has now been recognized as a limiting factor in the design of all present and future linacs. Unless a remarkable and unforeseeable breakthrough is made, electron and possibly also proton linac instabilities will have to be coped with, whenever a given combination of current, pulse length and accelerator length is exceeded. A number of remedies suggest themselves: slow-wave structure modifications, selective Q-reduction for the dangerous modes, staggering or scrambling of different accelerator sections, feedback, quadrupole focusing, higher order focusing, time varying focusing, noise reduction and hopefully others that have not been thought of yet. How the problem is treated will depend to a considerable extent on the type of linac under con-

struction, and economics. The brief discussion presented below outlines some of the advantages and disadvantages of the various remedies, admittedly as they are viewed by experience and calculations at SLAC. Fig. 11 is a summary of the SLAC current improvement program. It shows beam break-up gain as a function of beam current for a 1.5 μ sec pulse length. The fine horizontal line indicates the approximate blow-up level corresponding to a beam radius equal to the bore radius of the accelerator. It is seen that without focusing, barely eight milliamperes would be transmitted. A more realistic starting point for the discussion is the line labeled "original triplet focusing" which corresponded to the available focusing conditions on the accelerator at the end of the construction period, around September 1966. At that time, the maximum beam break-up threshold was 20 mA for a 1.5 μ sec pulse.

Structure Modifications, Selective Q-Reduction and Section Staggering

It has often been suggested that one of the appealing remedies for the SLAC accelerator would be to rebuild the front-end of the machine. This could be done by redesigning the constant-gradient sections so that the HEM_{11} mode resonances are reduced or displaced with respect to the rest of the machine. The reduction could be achieved by attempting to lower the Q of all the suspected modes, either by using a larger cut-off hole at both ends of the ten-foot sections or possibly by building C-band couplers into the sides of the disk-loaded waveguide which would lower the loaded Q of the cavities. The pass-band displacement could be obtained by using a different mode for the accelerating frequency, e.g. $\pi/2$ rather than $2\pi/3$. Surprisingly enough, at least in theory, Fig. 11 shows that such an "rf fix" in Sectors 1 and 2 (666 ft) would only yield a 25% improvement for a reduction by a factor of 10 in the interaction strength. Furthermore, it would be extremely expensive and would require a fairly long accelerator shutdown. For these reasons, this solution is not being contemplated for the time being. The designer should also be cautioned that even if the HEM_{11} mode could be eliminated entirely, other higher modes, either of the forward or backward type, will get excited at higher frequencies.

Another solution which is being adopted for shorter machines such as the MIT accelerator described at this conference¹⁷ and probably also the ALS machine in France¹⁸, is to build three or four different types of constant-gradient sections where the HEM_{11} pass-band is progressively shifted up in frequency. Thus, in principle, whatever modulation is picked up by the beam over a given length has no pass-band to interact with, further downstream. Presumably, staggering should be better than scrambling! Proton machines, because of their inherent tapered phase velocity, already benefit from this type of construction.

Feedback

Contrary to original expectations, the idea of

curing beam break-up at SLAC by feedback is not promising. Several schemes were tested, as described extensively in Reference 11, but they did not produce sufficient results. It appears that the basic difficulty stems from the fact that in a short-pulse accelerator, beam break-up is entirely in the transient regime. To be effective, the feedback chains must be very wideband, have very large gains (> 80 dB) and short group delays (< 50 nanoseconds). Since, in addition, several such chains are needed along the machine for correction in both the vertical and horizontal planes, the complexity of the system becomes overwhelming and the cost prohibitive. On the other hand, feedback schemes may be more promising for c-w superconducting machines. For the moment, estimates made by Helm⁴ indicate that a 100 μ A c-w accelerator of the Stanford Mark III type would not suffer from break-up if the Q of the HEM₁₁ mode could be kept under 10⁷. However, if these conditions were not to hold or the current had to be increased, a feedback system could probably be made to cure the problem.

Focusing

The original SLAC focusing system¹ consisted of quadrupole triplets at the end of every sector (333-1/3 ft.). This system was strong enough to operate at $k_B S = \pi/2$ up to an energy of only 7 GeV or a length of 1/3 of the machine. Examples of beam break-up thresholds as a function of $k_B S$ have already been shown in Fig. 8. As discussed elsewhere¹¹, triplets had been selected because they produce less steering than doublets of the same length in case of alignment drifts and instabilities. Subsequently, it was found that the mechanical stability of the drift sections supporting the triplets was better than expected and that the two outer lenses, rewired as a doublet, gave a perfectly satisfactory focusing system of equivalent strength. With this scheme, two new quadrupole deployment plans could be achieved. First, the larger middle quadrupoles could be removed and used to build stronger doublets as shown in Fig. 12a. This plan is now well underway. It will allow operation at $k_B S \sim \pi/2$ at full energy over the full length of the accelerator. The resulting break-up threshold as shown in Fig. 11 should be of the order of 32 mA. Second, the smaller lenses, obtained through replacement by the larger ones, are being installed as singlets, every 40 ft., in the first six sectors, as shown in Fig. 12b. The resulting stronger focusing in the low energy region where the rate of growth is most rapid, should yield a break-up threshold of the order of 50 mA, the current originally specified for the SLAC machine. Experiments performed recently with a combination of these two schemes, both still incomplete, have yielded a threshold at full energy of about 30 mA.

The use of sextupoles, octupoles and time-varying quadrupoles has also been considered. Non-linear focusing was expected to produce HEM₁₁ phase reversal and mixing as a function of length by causing electron bunches at different radial distances from the axis to cross over at different

distances downstream of the magnet. Time-varying quadrupoles were to produce the same effect as a function of time within each 1.5 μ sec pulse. Computer calculations have shown, however, that neither one of these schemes is promising: on the one hand, it is necessary to introduce appreciable focusing changes over each e-folding distance to reduce the gain; on the other hand, if the percentage of lens modulation in space or in time is too large, the resulting over- or under-focusing spoils the beam transmission through the accelerator.

In conclusion, it should be said that the strong focusing quadrupole system now offers the best straightforward remedy to beam break-up at SLAC. Some of the other remedies discussed here are certainly applicable to other machines but future accelerator builders should try to reserve ample space along their beam axis for extra focusing elements in case all other schemes should be insufficient.

Acknowledgements

The work presented here and particularly the experimental results were made possible thanks to the collaboration of a large number of SLAC associates. The author is indebted to all of them. In particular, he wishes to thank R. F. Koontz and E. V. Farinholt for much of the recent data, R. H. Helm for all the computer verifications and R. H. Miller for many helpful discussions and suggestions.

References

1. For a comprehensive if perhaps not complete list of references on beam break-up see: R. H. Helm "Computer Study of Wave Propagation, Beam Loading and Beam Blowup in the SLAC Accelerator," LASL Linac Conference, Los Alamos, New Mexico (1966).
2. W. K. H. Panofsky, "Transient Behavior of Beam Breakup," SLAC Internal Report TN-66-27, Stanford Linear Accelerator Center, Stanford, California (1966).
3. R. L. Gluckstern "A Note on Transverse Beam Instabilities in Multisection Linacs," LASL Linac Conference, Los Alamos, New Mexico (1966).
4. R. H. Helm, "Preliminary Estimate of Beam Blowup for a Superconducting Electron Linac," SLAC Internal Report TN-67-6, Stanford Linear Accelerator Center, Stanford, California (1967).
5. M.L. Report No. 581, W. W. Hansen Laboratories of Physics, Stanford University, Stanford, California (February 1959).
6. M. C. Kelliher and R. Beadle, "Pulse Shortening in Electron Linear Accelerators," Nature 187, 1099 (1960).
7. J. C. Nygard and R. F. Post, "Recent Advances in High Power Microwave Electron Accelerators for Physics Research," Nuclear Instrum. and Methods, 1961, 2, p. 126.
8. M. C. Crowley-Milling, et al, "Pulse Shortening in Electron Linear Accelerators," Nature, 1961, 191, p. 483.

LOEW: ELECTRON LINAC INSTABILITIES

9. K. L. Brown, et al, "Linear Electron Accelerator Progress at Stanford University," International Conference on High Energy Accelerators, Brookhaven, 1961.
10. For a list of references on the TM_{11} -like or HEM_{11} mode, see for example: O. H. Altenmueller, et al, "Investigations of Traveling Wave Separators for the Stanford Two-Mile Linear Accelerator," SLAC Report No. 17, Stanford Linear Accelerator Center, Stanford, California (1963).
11. O. H. Altenmueller, et al, "Beam Break-Up Experiments at SLAC," LASL Linac Conference, Los Alamos, New Mexico (1966).
12. P. B. Wilson, HEPL Report No. 297, High Energy Physics Laboratory, Stanford University, Stanford, California.
13. R. P. Borghi, et al, "Design and Fabrication of the Accelerating Structure for the Stanford Two-Mile Accelerator," Advances in Microwaves, Vol. 1 (Academic Press Inc., New York), 1966.
14. In addition to R. H. Helm, contributions to the computer calculation at SLAC have also been made by W. B. Herrmannsfeldt and J. R. Rees.
15. M. Bander, "Solution of the Beam Break-Up Equation," SLAC Internal Report TN-66-28, Stanford Linear Accelerator Center, Stanford, California (1966).
16. Calculations made by R. H. Miller, private communication.
17. W. Bertozi, et al, "The MIT High Duty, High Intensity 400-MeV Linear Electron Accelerator," published in Proceedings of the IEEE Conference, March 1-3, 1967.
18. H. Lebouet, "Auto-Déflexion du Faisceau d'Un Accélérateur Linéaire," Rapport Interne, INT. 2217-HL/ml/md, CSF, France (1966).

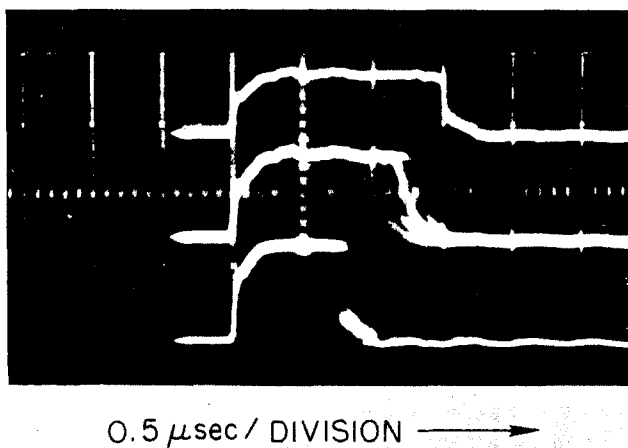


Fig. 1a. Beam pulses below and above break-up threshold.

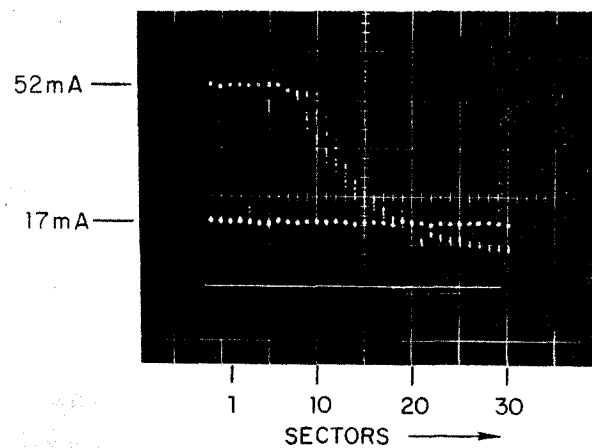


Fig. 1b. Transmitted beam profiles below and above break-up threshold (energy: 10 GeV, Pulse length: 1.6 μ sec).

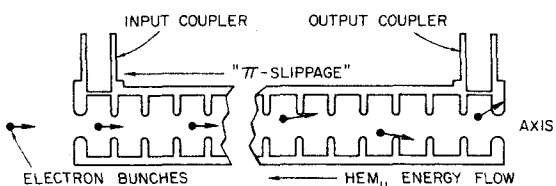


Fig. 2a. Single accelerator section showing regenerative instability.

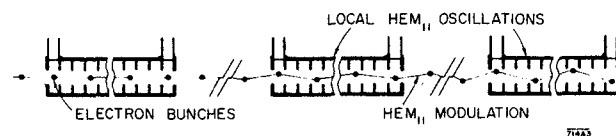


Fig. 2b. Multi-section accelerator showing cumulative instability build-up.

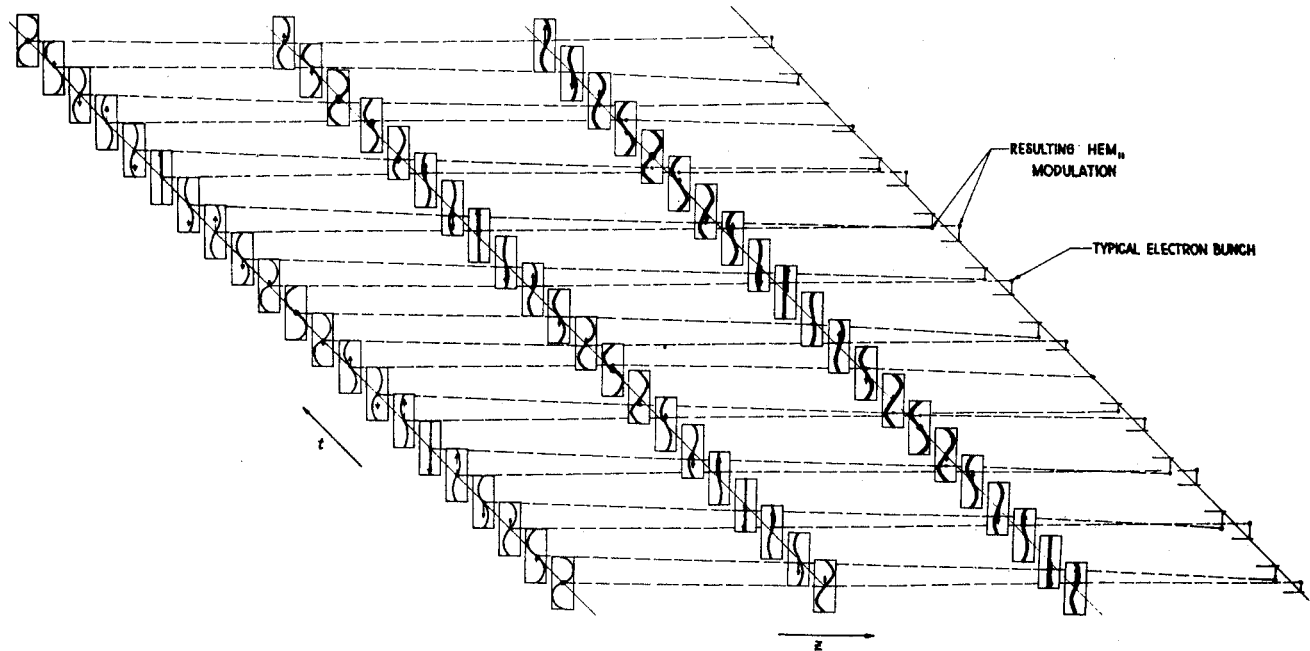


Fig. 3. Snapshots of three different cavities excited in HEM₁₁-mode at times of bunch passage. Arrow in cavity indicates momentum impulse.

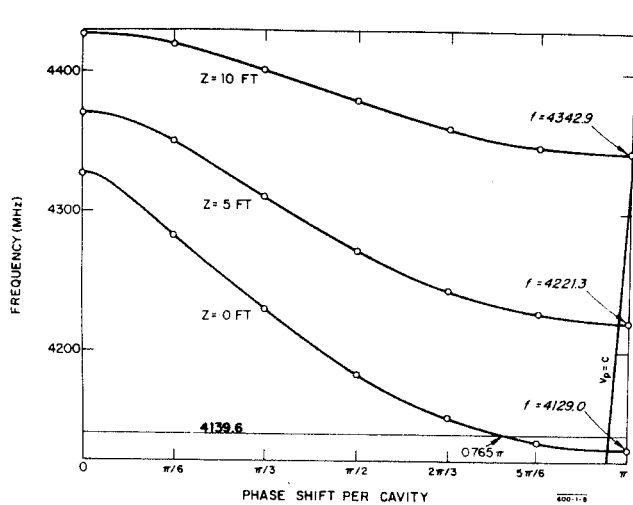
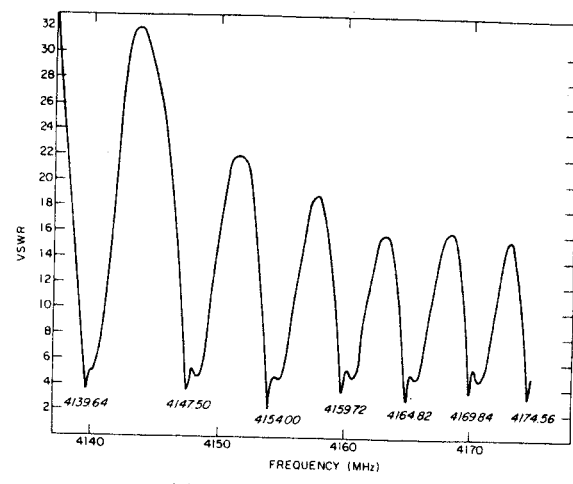


Fig. 4. Brillouin diagrams for HEM₁₁-mode at three locations in constant-gradient section.



(a) VSWR LOOKING INTO SECTION INPUT

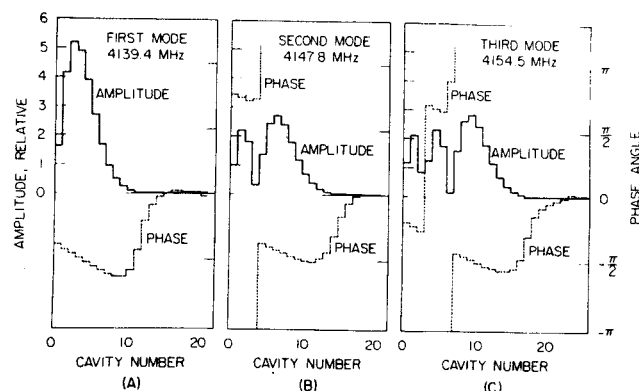


Fig. 5. Measured and computed HEM₁₁-mode resonances in SLAC constant-gradient section.

LOEW: ELECTRON LINAC INSTABILITIES

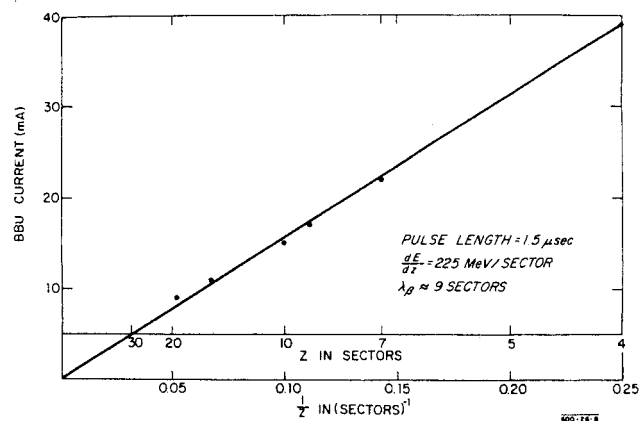


Fig. 6a. Beam break-up current vs. inverse length.

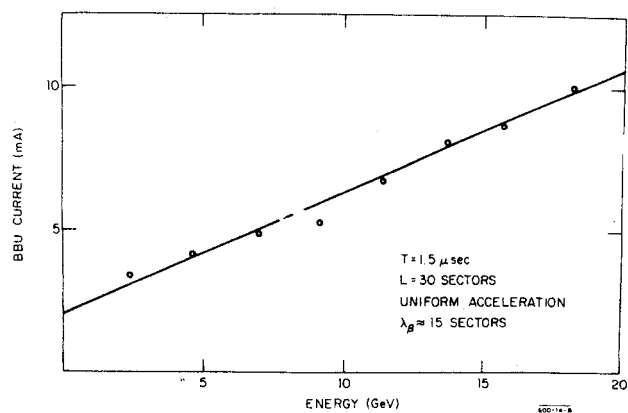


Fig. 6b. BBU current vs. energy.

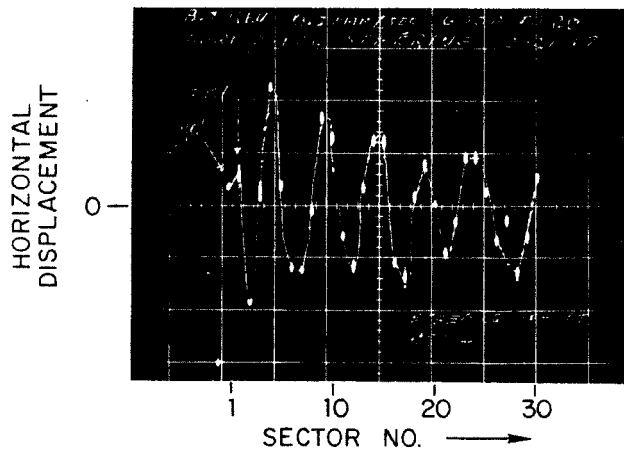


Fig. 7. Typical beam trajectory showing betatron oscillations. Dots indicate horizontal position of beam at end of each sector with steering off at 40 ft. point ($E = 8.7$ GeV, quadrupole current taper = 0.5 ampere/sector up to sector 20, $\lambda_B \sim 5$ sectors).

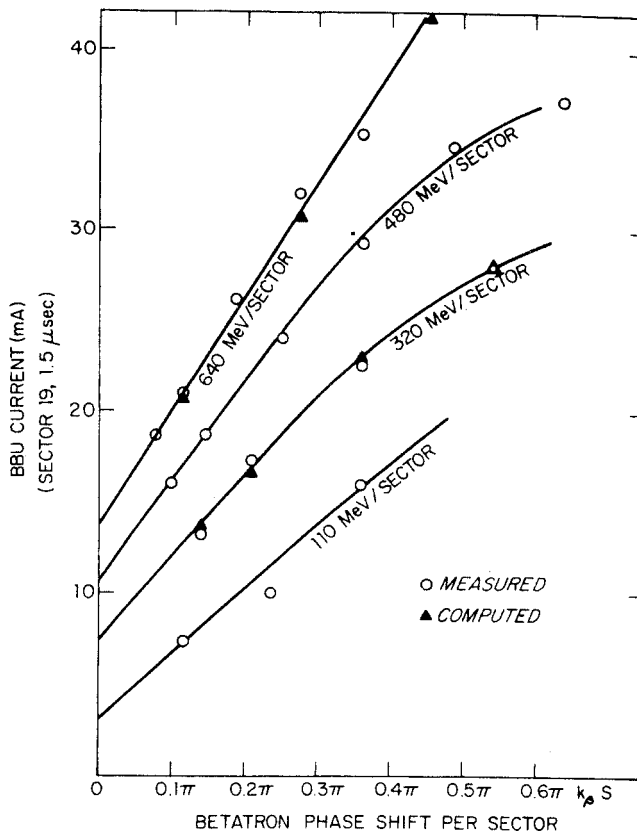


Fig. 8. Beam break-up current vs. betatron phase shift per sector (sector 19, 1.5 μ sec).

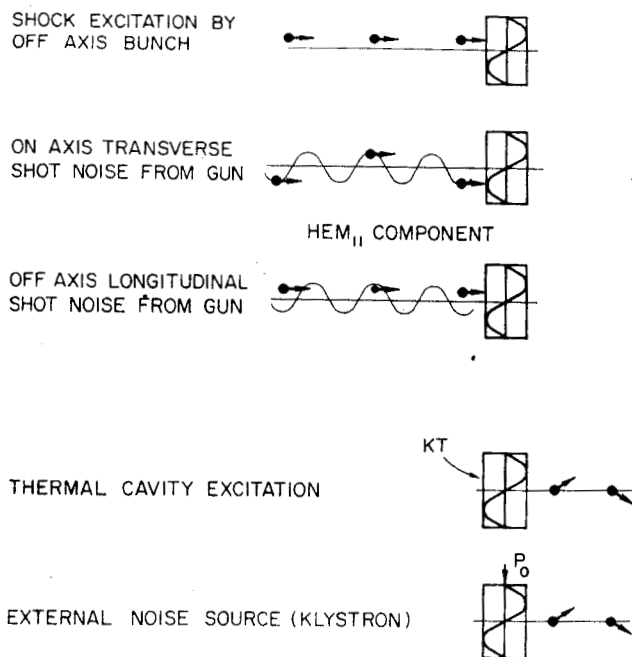


Fig. 9. Beam break-up noise sources.

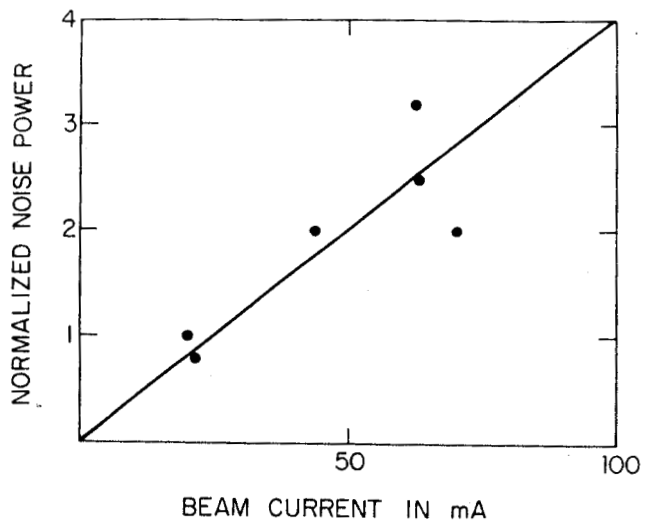


Fig. 10. Starting noise power vs. beam current.

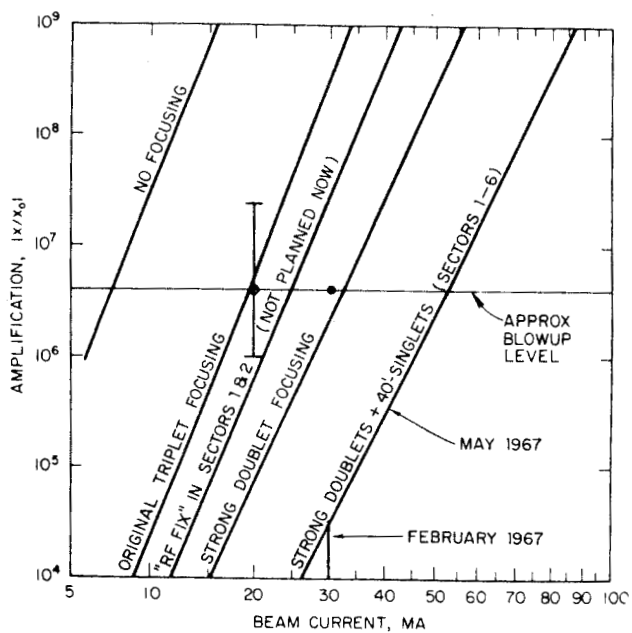


Fig. 11. Summary of SLAC beam transmission improvement program.

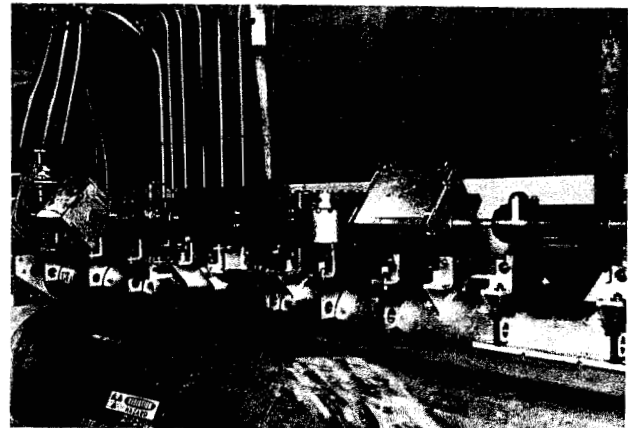


Fig. 12a. New strong quadrupole doublets.

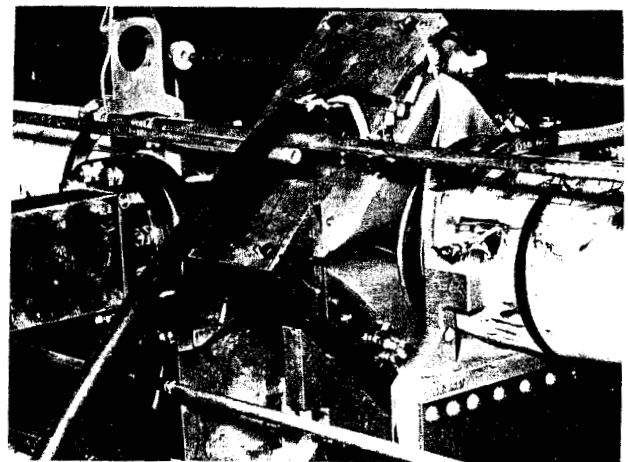


Fig. 12b. New 40 ft. spaced singlet (sectors 1-6).